Comprehensive Evaluation of Rapamycin's Specificity as an mTOR Inhibitor

Filippo Artoni[1,2], Nina Grützmacher[1], Constantinos Demetriades[1,2,3,§]

[1]Max Planck Institute for Biology of Ageing (MPI-AGE), 50931 Cologne, Germany

[2]Cologne Graduate School of Ageing Research (CGA), 50931 Cologne, Germany

[3]University of Cologne, Cologne Excellence Cluster on Cellular Stress Responses in Aging-Associated Diseases (CECAD), 50931 Cologne, Germany

[§]Correspondence: Demetriades@age.mpg.de (C.D.)

Running Title: Rapamycin specifically inhibits mTOR

Abstract

Rapamycin is a macrolide antibiotic that functions as an immunosuppressive and anti-cancer agent, and displays robust anti-ageing effects in multiple organisms including humans. Importantly, rapamycin analogs (rapalogs) are of clinical importance against certain cancer types and neurodevelopmental diseases. Although rapamycin is widely perceived as an allosteric inhibitor of mTOR (mechanistic target of rapamycin), the master regulator of cellular and organismal physiology, its specificity has not been thoroughly evaluated so far. In fact, previous studies in cells and in mice suggested that rapamycin may be also acting independently from mTOR to influence various cellular functions. Here, we generated a gene-edited cell line, that expresses a rapamycin-resistant mTOR mutant ($mTOR^{RR}$), and assessed the effects of rapamycin treatment on the transcriptome and proteome of control or $mTOR^{RR}$-expressing cells. Our data reveal a striking specificity of rapamycin towards mTOR, demonstrated by virtually no changes in mRNA or protein levels in rapamycin-treated $mTOR^{RR}$ cells, even following prolonged drug treatment. Overall, this study provides the first comprehensive and conclusive assessment of rapamycin's specificity, with important potential implications for ageing research and human therapeutics.

Keywords

rapamycin / sirolimus / mTORC1 / ageing / proteomics

Introduction

Rapamycin (also known as Sirolimus) is a naturally-occurring macrolide compound which was originally isolated from soil bacteria on Easter Island (Rapa Nui) in 1972 (Benjamin *et al*, 2011; Arriola Apelo & Lamming, 2016; Li *et al*, 2014). Rapamycin was primarily used in the clinic as an anti-fungal agent until 1999 when it was approved by the FDA for the prevention of kidney transplant rejection and later for the treatment of advanced kidney cell carcinoma. Its immunosuppressive and anti-proliferative properties are thought to be largely mediated by inhibition of mTOR, a serine/threonine kinase that functions as the master regulator of most cellular functions, including immune cell activation and cell growth control (Arriola Apelo & Lamming, 2016; Benjamin *et al.*, 2011; Fernandes & Demetriades, 2021; Li *et al.*, 2014). At the molecular level, rapamycin inhibits mTORC1 (mTOR complex 1) activity as a complex with the cytosolic immunophilin FKBP12 (FK506-binding protein 12). Binding of this drug-protein complex to mTOR blocks access to its catalytic site and prevents the phosphorylation of key substrates like S6K (ribosomal protein S6 kinase) (Chung *et al*, 1992). Additional immunophilins such as FKBP12.6, FKBP51, and FKBP52 have also been reported to bind and shape the pharmacology of rapamycin (Marz *et al*, 2013).

Over the last two decades, rapamycin has gained renewed interest after multiple studies uncovered its powerful anti-ageing properties (Arriola Apelo & Lamming, 2016; Benjamin *et al.*, 2011; Fernandes & Demetriades, 2021; Li *et al.*, 2014). Rapamycin has repeatedly been shown to extend lifespan and/or healthspan in worms (Robida-Stubbs *et al*, 2012), flies (Bjedov *et al*, 2010; Castillo-Quan *et al*, 2019; Schinaman *et al*, 2019), and mice (Bitto *et al*, 2016; Fok *et al*, 2014; Harrison *et al*, 2009). It extends chronological age in yeast (Powers *et al*, 2006) and reduces markers of senescence in cultured cells (Wang *et al*, 2017). More recently, studies conducted on marmoset monkeys have demonstrated rapamycin to have a good safety and tolerability profile (Lelegren *et al*, 2016; Tardif *et al*, 2015) thus paving the way for human

trials. Currently, trials are underway on both companion dogs (Creevy *et al*, 2022) and humans (NCT04488601) with preliminary evidence suggesting improvement in cardiac function in middle-aged dogs who received rapamycin for 10 weeks (Urfer *et al*, 2017). Notably, rapamycin extends lifespan at doses much lower than the ones used to achieve immunosuppression in transplant patients thus minimizing potential side effects. Finally, even transient, intermittent, or late-life rapamycin administration has been shown to extend lifespan in flies and mice thus making Rapamycin an attractive option for human use as an anti-ageing compound (Bitto *et al.*, 2016; Harrison *et al.*, 2009; Partridge *et al*, 2020).

The target specificity of rapamycin has recently been debated. On one hand, *in vitro* kinase activity assays showed other serine/threonine kinases, besides mTOR, to be largely insensitive to rapamycin up to concentrations at the micromolar range. Likewise, receptor-binding assays indicated that many ligand-receptor interactions remain unaffected by rapamycin, with the possible exception of histamine I binding (European Medicine Agency, 2005). On the other hand, accumulating evidence in the literature suggests that rapamycin may exert some of its effects via mTOR-independent mechanisms. This is also supported by the fact that most kinase inhibitors demonstrate very low target selectivity (Hantschel, 2015; Hantschel *et al*, 2012; Karaman *et al*, 2008). For instance, rapamycin was suggested to block the exercise-induced accumulation of ribosomal RNA (rRNA) in the skeletal muscle of both wild-type and mice containing a rapamycin-resistant mTOR allele (Goodman *et al*, 2011). Moreover, rapamycin and other rapalogs were shown to directly bind and activate the lysosomal mucolipin TRP channel (TRPML1; also known as MCOLN1) independently of mTOR inhibition (Zhang *et al*, 2019). Finally, since FKBPs serve as chaperones for proper folding of several proteins (Bonner & Boulianne, 2017; Bultynck *et al*, 2001; Galfre *et al*, 2012; Vervliet *et al*, 2015; Wang *et al*, 1996), it can be speculated that their binding to rapamycin may be influencing cellular physiology via altering the interaction of FKBPs to their client proteins.

Here, to comprehensively address this important unresolved issue, we generated a rapamycin-resistant cell line by editing a single base in the *MTOR* gene at its endogenous locus (Choi *et al*, 1996; Hosoi *et al*, 1999; Lorenz & Heitman, 1995) and assessed how rapamycin affected the cellular transcriptome and proteome in an unbiased manner. These experiments unraveled an impressive specificity of rapamycin towards mTOR, with the rapamycin effects on gene expression and protein levels being virtually non-existent in the mTOR-mutant cells.

Results

Generation and characterization of a gene-edited cell line that expresses rapamycin-resistant mTOR

Mutations in the mTOR FRB (FKBP-rapamycin-binding) domain that disrupt its interaction with FKBP12 and confer rapamycin resistance to mTOR have been described almost 30 years ago (Brown *et al*, 1995; Chen *et al*, 1995; Choi *et al.*, 1996; Lorenz & Heitman, 1995; Hara *et al*, 1997; Hosoi *et al.*, 1999). Although such mTOR mutants have been used in previous studies, usually expressed exogenously in cells or via transgenic expression in mouse tissues, the presence of endogenous wild-type mTOR has complicated the interpretation of such results (Ge *et al*, 2009; Goodman *et al.*, 2011; Luo *et al*, 2015; Zhang *et al*, 2000). Moreover, a comprehensive analysis of rapamycin's effects in such cellular models, beyond single readouts, is lacking. Therefore, to probe whether rapamycin also acts through mTOR-independent mechanisms or exclusively via mTOR inhibition, we used CRISPR/Cas9-mediated gene editing to generate a HEK293FT cell line that expresses a Ser2035Thr mTOR mutant (Fig. 1A and Fig. EV1) that was previously described to be rapamycin-resistant (Brown *et al.*, 1995; Chen *et al.*, 1995; Choi *et al.*, 1996; Lorenz & Heitman, 1995)(Hara *et al.*, 1997; Hosoi *et al.*, 1999). Intuitively, we called this mutant and the associated cell line, $mTOR^{RR}$ (mTOR rapamycin-resistant). Importantly, as we mutated *MTOR* in the endogenous locus, no wild-type mTOR is

expressed in these cells, verified by genomic DNA sequencing (Fig. EV1). Consistent with previous reports, the rapamycin-induced interaction of FLAG-tagged FKBP12 with wild-type mTOR, was completely abrogated in mTOR^{RR} (Fig. 1B). Of note, the catalytic activity of mTORC1 containing mTOR^{RR}, as assessed by the phosphorylation of its direct substrate S6K, was indistinguishable from that in control cells and was diminished by treatment with Torin1, an ATP-competitive mTOR inhibitor (Fig. 1C). In contrast, mTOR^{RR} demonstrated complete resistance to rapamycin even when cells were treated with this compound at micromolar concentrations (Fig. 1C), or when the treatment was extended to 24 or 48 hours (Fig. 1D). Similar to rapamycin, mTOR^{RR} also exhibited full resistance to other rapalogs like everolimus and temsirolimus (Fig. 1E), but responded properly to amino acid (AA) starvation, showing that the regulation of mTORC1 by other inhibitory stimuli is unperturbed in mTOR^{RR} cells (Fig. 1F). In sum, the mTOR^{RR} HEK293FT cell line is a 'clean', reliable and robust model to investigate rapamycin's specificity towards mTOR.

Rapamycin alters gene expression exclusively via mTOR inhibition

Having validated our experimental model, we then treated control (WT) and mTOR^{RR} cells with rapamycin for 24 hours and performed RNA-seq experiments to investigate its effects on global gene expression. In line with mTOR—directly or indirectly—regulating the activity of several transcription factors (Hardwick *et al*, 1999; Laplante & Sabatini, 2013), we detected more than 5000 genes whose expression changed significantly in WT cells upon rapamycin treatment (Fig. 2A,B and Suppl. Table 1). Our analysis identified several genes that are known to be affected by mTOR inhibition (e.g., HMOX1, RHOB, MYC) (Bayeva *et al*, 2012; Gordon *et al*, 2015; Jin *et al*, 2013; Sun *et al*, 2022; Visner *et al*, 2003) (Fig. 2B) thus validating our experimental setup. Similarly, rapamycin decreased the expression of AA transporters like SLC7A5 and SLC7A11, which are known to be regulated downstream of an mTORC1-ATF4 axis (Torrence *et al*, 2021) (Fig. 2B and Suppl. Tables 1, 2).

Gene ontology (GO) term enrichment analysis, using the differentially regulated genes that are strongly down- or upregulated by rapamycin ($Log_2FC < –0.75$ and $Log_2FC > +0.8$, respectively), revealed a strong enrichment of ribosome-related Biological Process (BP) and Cellular Component (CC) terms (e.g., BP:GO:0042254~ribosome biogenesis; CC:GO:0030684~preribosome) (Fig. 2C,D and Suppl. Table 2). Confirming the well-known role of mTOR in promoting ribosome biogenesis and positively regulating rRNA expression (Mayer & Grummt, 2006; Powers & Walter, 1999), all genes that fall under these terms (e.g., RRP12, RRP9, RRS1, RRP1, RPF2, NOP16, NOL6, DDX21, MRTO4, MRM1) were found to be downregulated by rapamycin (Fig. 2C,D and Suppl. Table 2). Interestingly, we also observed a strong enrichment of terms related to mitochondria-resident proteins (e.g., CC:GO:0005739~mitochondrion; CC:GO:0005759~mitochondrial matrix) and associated mitochondrial functions (e.g., BP:GO:0019752~carboxylic acid metabolic process) among the genes that are differentially regulated by rapamycin (Fig. 2C,D and Suppl. Table 2). Similar results were obtained when performing the GO analysis with more relaxed criteria including all significantly down- and upregulated genes, instead of setting cut-offs for those that change robustly upon rapamycin (Fig. EV2A,B and Suppl. Table 3). Strikingly, unlike the massive transcriptional effects of rapamycin in control cells, we found only 3 genes whose expression was altered in $mTOR^{RR}$ cells treated with rapamycin (Fig. 2A,B and Suppl. Table 1). These data indicated that rapamycin practically regulates transcription exclusively via its direct inhibitory effect on mTOR.

Rapamycin alters the cellular proteome exclusively through mTOR

In addition to their involvement in transcriptional regulation, the best-described role of rapamycin and mTORC1 is in the control of *de novo* protein synthesis via controlling the phosphorylation and activity of—direct or indirect—mTORC1 targets like S6K, 4E-BP1, and

S6, with only certain 4E-BP1 phospho-sites being rapamycin-sensitive (Thoreen *et al*, 2012; Thoreen *et al*, 2009). Therefore, we next sought to investigate the rapamycin-induced changes in the cellular proteome and to explore how much of this happens due to mTOR inhibition.

To this end, we treated control and mTOR^{RR} cells with rapamycin for 24 or 48 hours and performed whole-proteome quantitative mass spectrometry experiments. Out of a total of approximately 7500 proteins that were detected and quantified, the levels of more than 2500 and 2300 proteins changed significantly in WT cells treated with rapamycin for 24 or 48 hours, respectively (Fig. 3A-C and Suppl. Table 4). Similar to what we observed in transcriptomic analyses, these hits include multiple proteins belonging to pathways that have been previously described to be regulated by rapamycin and mTOR (e.g., PDCD4, RHOB, HMOX1, SQSTM1, PRELID1, SCD, SESN2) (Bayeva *et al.*, 2012; Dorrello *et al*, 2006; Gordon *et al.*, 2015; Jin *et al.*, 2013; Ko *et al*, 2017; Mauvoisin *et al*, 2007; Sun *et al.*, 2022; Visner *et al.*, 2003; Wall *et al*, 2008; Zhu *et al*, 2020) as well as several amino acid transporters (SLC7A11, SLC38A10, SLC3A2, SLC7A5) (Graber *et al*, 2017; Nachef *et al*, 2021; Torrence *et al.*, 2021; Zhang *et al*, 2021) (Fig. 3B,C and Suppl. Table 4). Remarkably, however, none of the 7574 detected proteins were differentially regulated in rapamycin-treated mTOR^{RR} cells, even after prolonged drug treatment (Fig. 3A-C and Suppl. Table 4), again showing complete absence of mTOR-independent effects by rapamycin.

Consistent with our observations from RNA-Seq experiments, GO analysis using all proteins that are significantly down- or upregulated ($p < 0.05$) upon 24-hour rapamycin treatment in WT cells showed strong enrichment of terms related to ribosomes and translation (e.g., BP:GO:0022613~ribonucleoprotein complex biogenesis; BP:GO:0042254~ribosome biogenesis; BP:GO:0006412~translation) (Fig. 3D and Suppl. Table 5) with the majority of proteins that belong to this category being downregulated (e.g., CDC123, CCRN4L, LTV1,

RRN3, EIF1AD, SESN2, GNL3L, CCDC86, WDR74, TNRC6A) (Fig. 3B,D and Suppl. Tables 4, 5). Another prominent group of GO terms that is enriched in the proteomic analysis includes terms related to the cell cycle (e.g., BP:GO:0007049~cell cycle, BP:GO:0000278~mitotic cell cycle) (Fig. 3D and Suppl. Tables 4, 5) with proteins being either down- or upregulated upon rapamycin treatment (e.g., CDC123, CDC6, ASNS, ECD, CEP72, PDCD4, RHOB, HMGN3, DHFR, TRIOBP) (Fig. 3D). Of note, this is in line with the well-established role of rapamycin and mTOR in the regulation of cell proliferation (Dowling *et al*, 2010). Similar results were obtained when analyzing the respective dataset (all significantly-regulated proteins; $p < 0.05$) from 48-hour rapamycin treatment in WT cells (Fig. 3A,C, Fig. EV3 and Suppl. Table 6).

Furthermore, in line with the robust expression changes in genes related to mitochondria (Fig. 2C,D), we observed similar effects in the levels of mitochondrial proteins, as shown by the strong enrichment of related GO terms (e.g., CC:GO:0005739~mitochondrion; CC:GO:0005759~mitochondrial matrix) (Fig. 3E and Suppl. Tables 4, 5). Interestingly, when performing the GO term analysis using only the strongly up- or downregulated proteins, the enrichment of terms related to mitochondrial proteins became even more prominent (Fig. EV4 and Suppl. Table 7) with most mitochondria-related proteins being upregulated by rapamycin (e.g., BNIP3, BNIP3L, CPS1, TXNRD2, SDSL, ACSF2, BPHL, HMGCL, HSD17B8, SFN) (Fig. EV4 and Suppl. Tables 4, 7).

Finally, although a connection between mTOR activity and cell adhesion has been described before, the underlying mechanisms are less clear (Asrani *et al*, 2017; Chen *et al*, 2015). Interestingly, our proteomics analysis showed that rapamycin treatment led to significant changes in the levels of a large number of proteins that are related to adherens and anchoring junctions (CC:GO:0005912~adherens junction; CC:GO:0070161~anchoring junction), most of which are downregulated under these conditions (e.g., GJA1, SLC3A2, RANGAP1, DSP,

FASN, APC, EEF2, EIF2A, TNKS1BP1, ATXN2L) (Fig. 3B,E and Suppl. Tables 4, 7). This suggests that some of the effects of rapamycin/mTOR on cell adhesion may stem from changes in the junctional proteome.

In sum, our unbiased interrogation of rapamycin's effects in cells reveals an extraordinary specificity of this compound towards mTOR, and—at the same time—provides a comprehensive evaluation of its role on the cellular transcriptome and proteome.

Discussion

According to previous studies, the majority of inhibitory compounds that are used in research or in therapeutics demonstrate off-target effects, influencing the activity of additional signaling molecules that can also be structurally-unrelated to their presumed targets. Sometimes, inhibitors even show higher potency towards off-targets compared to on-target effects (Davies *et al*, 2000; Bain *et al*, 2003; Bain *et al*, 2007; Fedorov *et al*, 2007; Davis *et al*, 2011). In fact, very few FDA-approved kinase inhibitors have demonstrated high target selectivity, whereas the majority influences the activity of 10-100 off-target kinases (Hantschel, 2015; Hantschel *et al*, 2012; Karaman *et al*, 2008). Importantly, the low specificity and selectivity of most kinase inhibitors greatly complicates the interpretation of data originating from their use and has important implications for their applicability in both research and therapeutics.

Surprisingly, although rapamycin has been used as an mTOR inhibitor for more than three decades, its specificity towards this key signaling hub has not been thoroughly evaluated so far. In fact, previous studies have hinted at the existence of mTOR-independent functions of rapamycin in cells and in transgenic mouse models thus underscoring the need for a detailed evaluation of its specificity. In transgenic mice overexpressing a rapamycin-resistant mTOR mutant in skeletal muscles, rapamycin was still able to partially suppress mechanical-loading-

induced ribosome biogenesis (Goodman *et al.*, 2011). It is worth noting however, that these transgenic mice were maintained as hemizygotes with the mTOR^{RR} allele expressed on top of endogenous wild-type mTOR (Ge *et al.*, 2009; Goodman *et al.*, 2011), which does not allow for safe conclusions to be drawn from such experiments. Indeed, the observed rapamycin effects that were previously interpreted as mTOR-independent can also be ascribed to the inhibition of endogenous wild-type mTOR molecules. This is also supported by our findings, using a gene-edited cell line that expresses mutant, rapamycin-resistant mTOR from the endogenous *MTOR* locus, while lacking expression of wild-type mTOR: unlike the previously-described mTOR^{RR} transgenic mice, our mTOR^{RR} cells are fully resistant to rapamycin, which is demonstrated by unaffected mTORC1 activity, diminished FKBP12-mTOR binding, and complete lack of transcriptional or proteomic changes in response to rapamycin treatment.

A more recent study reported that micromolar concentrations of rapamycin (or of other rapalogs like everolimus and temsirolimus) can directly bind to TRPML1/MCOLN1, the primary lysosomal calcium release channel, and enhance its activity in an mTOR-independent manner (Zhang *et al.*, 2019). Although rapalogs may indeed act on additional substrates at such concentrations, these are two to three orders of magnitude higher than those classically used in cell culture experiments (2-20 nM; like those we used for the transcriptomic and proteomic analyses described here) or—most importantly—those that are detected in the blood of patients that take rapamycin. More specifically, whole-blood concentrations (WBC) of rapamycin/sirolimus are in the 10-20 nM range in renal transplant patients to prevent graft rejection (Meier-Kriesche & Kaplan, 2000). In patients treated with everolimus against metastatic renal cell carcinoma, the median WBC is approximately 15 nM (Takasaki *et al*, 2019), while plasma concentrations of temsirolimus for relapsed/refractory multiple myeloma average around 9 nM (Farag *et al*, 2009). Higher doses of temsirolimus have only been used as a last resort in clinical trials against aggressive forms of lymphoma with WBC values reaching

500-600 nM (Hudes *et al*, 2007), which is still more than 25 times lower than the rapamycin concentration required to half-maximally activate TRPML1 (Zhang *et al.*, 2019). Thus, the rapamycin-mediated TRPML1 activation, while observed *in vitro*, is not likely to be physiologically relevant for research and therapeutics. Furthermore, rapamycin doses aimed at slowing or reversing ageing are generally even lower than those used for immunosuppression and cancer treatment (Bitto *et al.*, 2016; Bjedov *et al.*, 2010; Castillo-Quan *et al.*, 2019; Fok *et al.*, 2014; Harrison *et al.*, 2009; Robida-Stubbs *et al.*, 2012; Schinaman *et al.*, 2019), further suggesting that TRPML1 activation is unlikely to be involved in rapamycin-mediated lifespan extension.

Rapamycin acts an allosteric mTOR inhibitor in a complex with FKBP12 and other FKBP family members (Chung *et al.*, 1992; Marz *et al.*, 2013). Most FKBPs possess peptidyl-prolyl isomerase (PPIase) activity, hence functioning as protein folding chaperones for a variety of different proteins (Harrar *et al*, 2001; Kolos *et al*, 2018). For instance, FKBP12 and FKBP12.6 have been shown to bind and modulate the activity of ryanodine receptors (RyRs) and inositol 1,4,5-trisphosphate receptors (IP3Rs) (Bultynck *et al.*, 2001; Galfre *et al.*, 2012; Vervliet *et al.*, 2015), which are channels involved in intracellular calcium release. FKBP12 has also been shown to inhibit TGFβ family type I receptors (Wang *et al.*, 1996). Likewise, the larger FKBP51 and FKBP52 chaperones control glucocorticoid receptor (GR) localization and activity (Fries *et al*, 2017) as well as the protein levels of Argonaute 2 (AGO2) (Martinez *et al*, 2013), an essential component of the RNA-induced silencing complex (RISC). Hence, it would be reasonable to speculate that binding of rapamycin to different FKBP proteins may influence the folding—and thus function—of client proteins, also beyond mTOR inhibition. Because any changes in receptor or signaling pathway activities, organelle function, metabolism, or other cellular processes are eventually translated to changes in gene or protein expression, we here analyzed the cellular transcriptome and proteome to interrogate the effects of rapamycin

314 treatment in an unbiased manner. These experiments revealed a striking dependence of
315 rapamycin on mTOR inhibition to influence cells, with mTOR^{RR}-expressing cells
316 demonstrating virtually no effects upon treatment with this drug. In sum, although rapamycin
317 could—in theory—affect cells also independently from mTOR inhibition (via TRPML1 or
318 through FKBP-dependent mechanisms), this is not the case, at least for rapamycin
319 concentrations that are within the nanomolar range used in research or found in the blood of
320 patients treated with this drug or its analogs.
321
322 In addition to assessing rapamycin's specificity towards mTOR, we here also investigated how
323 rapamycin influences gene expression and whole-cell protein levels in control cells that express
324 wild-type mTOR. Consistent with the role of mTORC1 in regulating cap-dependent translation
325 (Fonseca *et al*, 2014; Holz *et al*, 2005; Liu & Sabatini, 2020; Ma & Blenis, 2009; Thoreen *et*
326 *al.*, 2012) and with rapamycin's ability to repress both global and specific translation of key
327 subsets of transcripts (Dickinson *et al*, 2011; Huo *et al*, 2011; Nandagopal & Roux, 2015;
328 Tsukumo *et al*, 2016; Wang *et al*, 2007), these transcriptomics and proteomics datasets
329 identified several thousands of genes and proteins whose expression changes in rapamycin-
330 treated cells. For instance, highlighting the well-described role of rapamycin/mTOR on
331 ribosomal biogenesis, rapamycin treatment strongly downregulated the expression of genes
332 encoding for ribosomal proteins, tRNA synthetases (Kim *et al*, 2017; Lee *et al*, 2012) and other
333 accessory proteins involved in this process (Mayer & Grummt, 2006; Powers & Walter, 1999)
334 (Fig. 2 and EV2). Accordingly, we observed a strong enrichment of proteins related to non-
335 coding RNA metabolic processes and ribonucleoprotein complex biogenesis among those
336 downregulated by rapamycin (Fig. 3 and EV3). Furthermore, both our RNA-seq and proteomics
337 data also confirm previous studies about rapamycin's role in regulating mitochondrial function
338 (Morita *et al*, 2017; Ramanathan & Schreiber, 2009; Rosario *et al*, 2019; Schieke *et al*, 2006;
339 Villa-Cuesta *et al*, 2014) (Fig. 2, 3 and EV2, 3). Interestingly, we find that proteins that are

340 associated with adherens/anchoring junctions are enriched among those downregulated by
341 rapamycin, which may suggest a role for mTOR in the regulation of cell-cell and cell-matrix
342 contacts (Fig. 3E and EV3B). Finally, we observe an enrichment of terms associated with cell
343 cycle and mitosis in the rapamycin-dependent proteome, possibly reflecting the anti-
344 proliferative effects of rapamycin (Zaragoza *et al*, 1998) and the role of mTOR in cell
345 proliferation (Dowling *et al.*, 2010).
346
347 Overall, we here provide an unbiased, comprehensive evaluation of rapamycin's specificity
348 towards mTOR in mammalian cells, in unprecedented depth. Given the immense potential that
349 rapamycin and its analogs have as anti-ageing compounds or in therapeutics, these findings
350 provide important insight for both basic and translational research and aim at improving the
351 applicability and specificity of its use in humans.
352

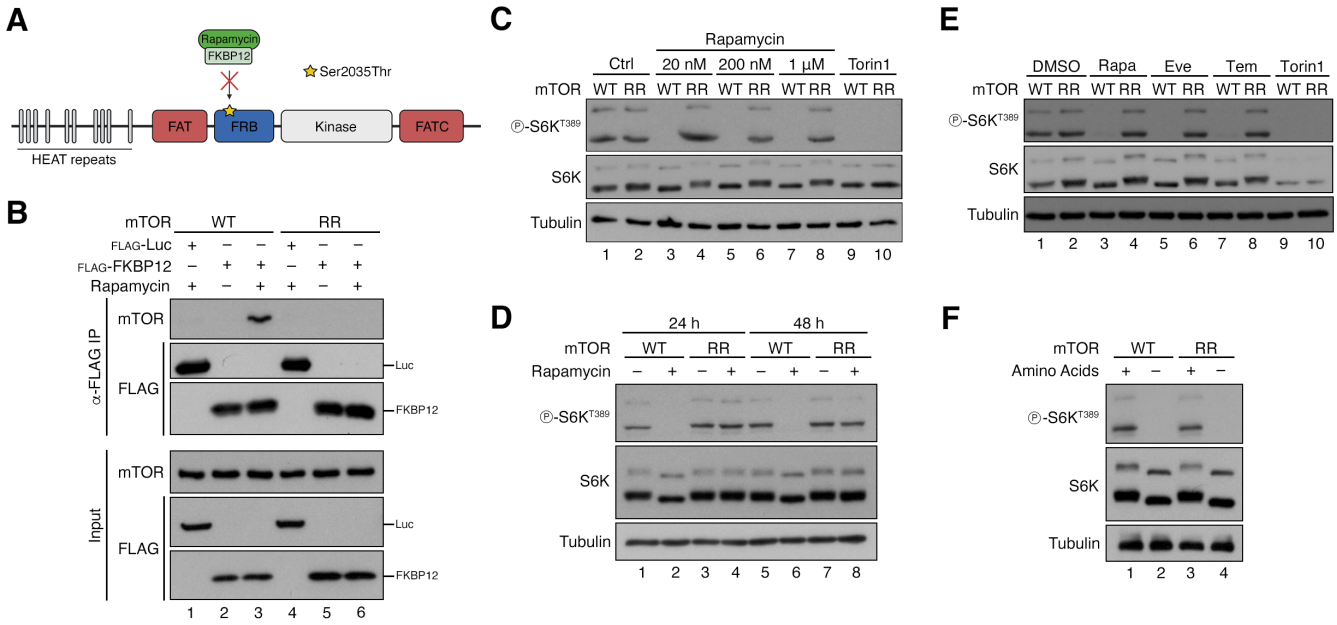

Figure 1. Generation and characterization of a gene-edited cell line that expresses rapamycin-resistant mTOR.

(A) Schematic model of the mTOR protein depicting key domains and the location of the Ser2035Thr substitution in the FRB domain that prevents its inhibition by rapamycin/FKBP12.

(B) Diminished binding of FKBP12 to the mTOR^{RR} mutant protein. Co-immunoprecipitation experiments in control (WT) or mTOR^{RR} HEK293FT cells, transiently expressing FLAG-tagged FKBP12 or Luciferase (Luc) as negative control, treated with rapamycin (20 nM, 1 h) or DMSO. Binding of mTOR to FKBP12 was analyzed by immunoblotting as indicated.

(C) mTOR^{RR} does not respond to rapamycin even at extremely high concentrations. Immunoblots with lysates from HEK293FT WT and mTOR^{RR} cells treated for 1 h with 20 nM to 1 μM rapamycin as indicated, 250 nM Torin1, or DMSO as control. mTORC1 activity was assessed by S6K phosphorylation.

(D) mTOR^{RR} is resistant to long-term rapamycin treatment. Immunoblots with lysates from HEK293FT WT and mTOR^{RR} cells treated with DMSO or rapamycin (20 nM) for 24 or 48 h, probed with the indicated antibodies.

(E) mTOR^{RR} shows resistance to multiple rapalogs. Immunoblots with lysates from HEK293FT WT and mTOR^{RR} cells treated with DMSO, rapamycin (Rapa; 20 nM), everolimus (Eve; 20 nM), temsirolimus (Tem; 20 nM), or Torin1 (250 nM) for 1 h, probed with the indicated antibodies.

(F) Cell expressing mTOR^{RR} have active mTORC1 that responds properly to AA starvation. Immunoblots with lysates from HEK293FT WT and mTOR^{RR} cells treated with control (+) or AA-free media (–) for 1 h, probed with the indicated antibodies.

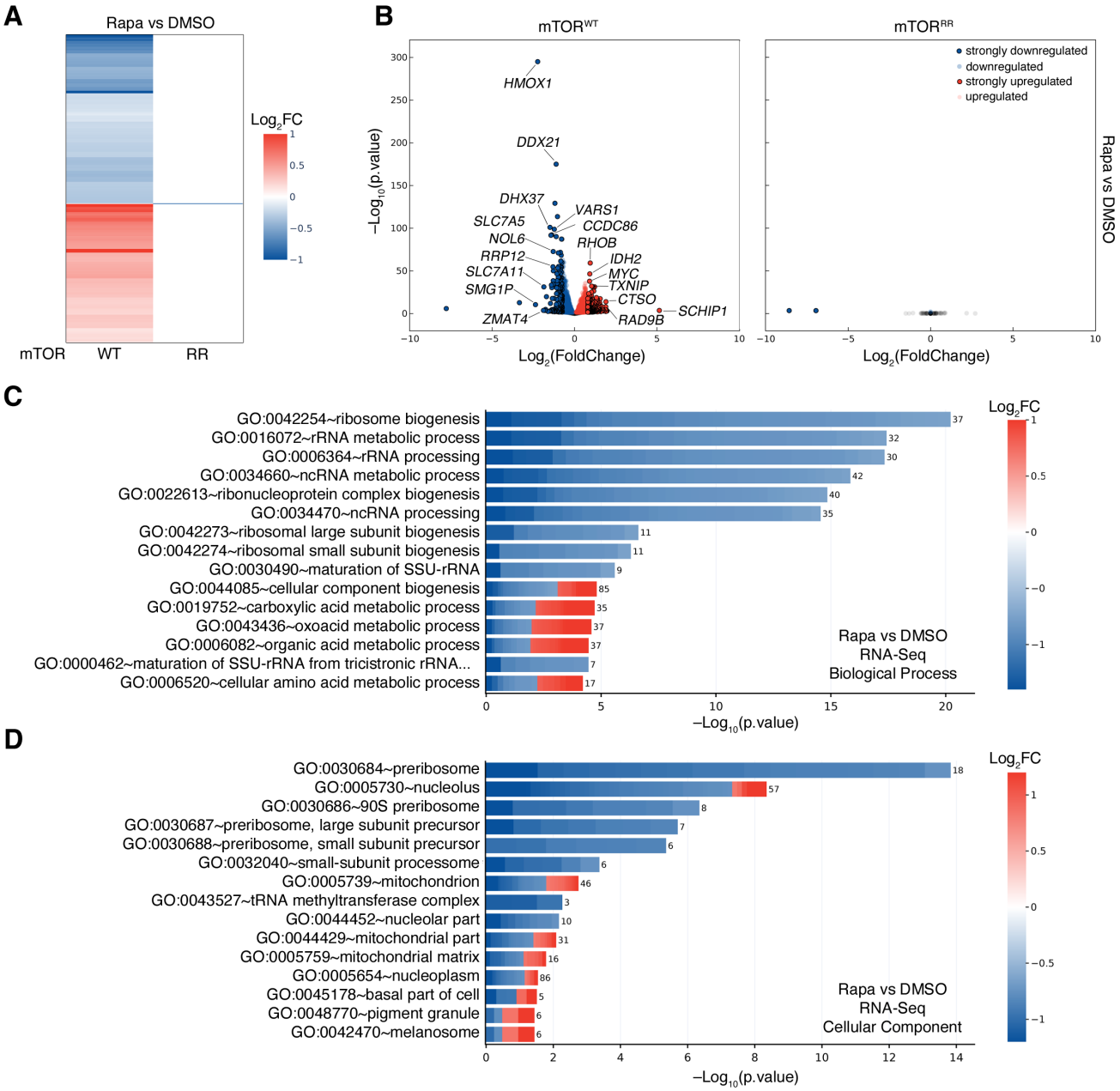

Figure 2. Rapamycin alters gene expression exclusively via mTOR inhibition.

(A) Heatmap depicting the rapamycin-induced changes in gene expression in HEK293FT WT and mTOR^{RR} cells. RNA-Seq data from cells treated with rapamycin (20 nM, 24 h) expressed as log-transformed fold change (Log_2FC). Only statistically-significant changes ($p < 0.05$) are shown.

(B) Volcano plots showing the rapamycin-induced changes in gene expression in HEK293FT WT (left) and mTOR^{RR} (right) cells from the RNA-Seq experiment described in (A). Genes that are significantly ($p < 0.05$) down- or upregulated by rapamycin are shown in blue or red

386 respectively. Strongly down- ($Log_2FC < –0.75$) or upregulated ($Log_2FC > +0.8$) genes are
387 shown with black outline. Unaffected genes ($p > 0.05$) shown as grey dots. Selected genes are
388 marked in the plot.
389 **(C)** Biological process (BP) GO term analysis using the genes that are strongly down- (blue) or
390 upregulated (red) by rapamycin in WT cells as described in (B). The color of each box in the
391 cell plot represents log-transformed fold change values for each gene in rapamycin- vs DMSO-
392 treated cells. The number of genes in the selected dataset for each GO term is shown on the
393 right side of each bar.
394 **(D)** As in (C), but for Cellular Component (CC) GO term analysis.
395

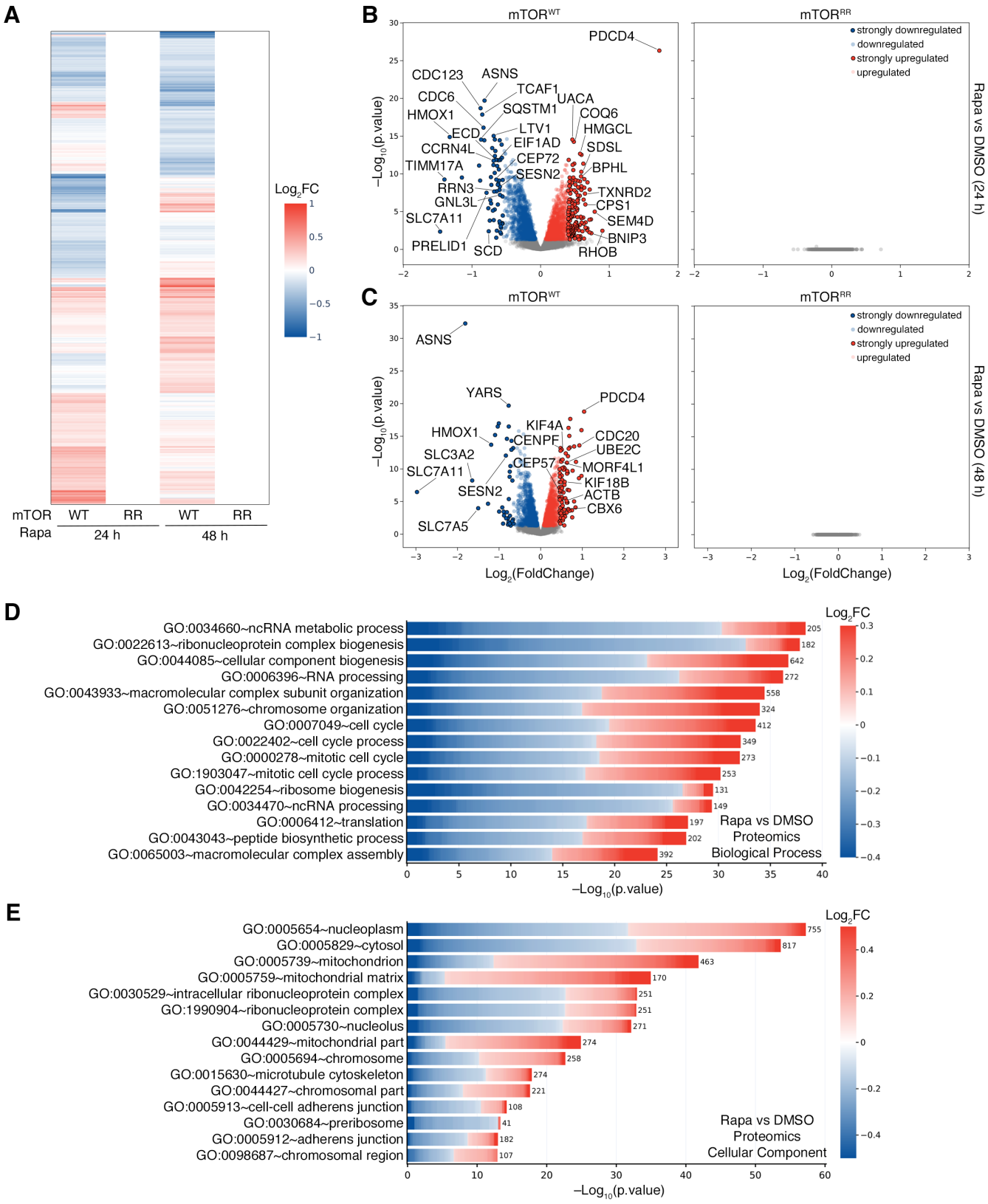

Figure 3. Rapamycin alters the cellular proteome exclusively via mTOR inhibition.

(A) Heatmap depicting the rapamycin-induced changes in the proteome of HEK293FT WT and mTOR^{RR} cells. Shown are whole-proteome quantitative mass-spectrometry data from cells

treated with rapamycin (20 nM) for 24 or 48 h expressed as log-transformed fold change (Log_2FC). Only statistically-significant changes ($p < 0.05$) are shown.

(B) Volcano plots showing the rapamycin-induced proteomic changes in HEK293FT WT (left) and $mTOR^{RR}$ (right) cells from the mass-spectrometry experiment described in (A). Proteins that are significantly ($p < 0.05$) down- or upregulated by rapamycin (20 nM, 24 h) are shown in blue or red respectively. Most strongly down- ($Log_2FC < –0.55$) or upregulated ($Log_2FC > +0.4$) proteins are shown with black outline. Unaffected proteins ($p > 0.05$) shown as grey dots. Selected proteins are marked in the plot.

(C) As in (B), but for cells treated with 20 nM rapamycin (or DMSO) for 48 h. Strongly down- ($Log_2FC < –0.65$) or upregulated ($Log_2FC > +0.45$) proteins are shown with black outline.

(D) Biological process (BP) GO term analysis using the proteins that are significantly down- (blue) or upregulated (red) by 24 h rapamycin in WT cells as described in (B). The color of each box in the cell plot represents log-transformed fold change values for each protein in rapamycin- vs DMSO-treated cells. The number of proteins in the selected dataset for each GO term is shown on the right side of each bar.

(E) As in (D), but for Cellular Component (CC) GO term analysis.

Methods

Cell culture

All cell lines were grown at 37 ºC, 5% CO_2. Human female embryonic kidney HEK293FT cells (#R70007, Invitrogen; RRID: CVCL_6911) were cultured in high-glucose Dulbecco's Modified Eagle Medium (DMEM) (#41965-039, Gibco) supplemented with 10% fetal bovine serum (FBS) (#F7524, Sigma, or #S1810, Biowest) and 1% Penicillin-Streptomycin (#15140-122, Gibco).

HEK293FT cells were purchased from Invitrogen. The identity of the HEK293FT cells was validated by the Multiplex human Cell Line Authentication test (Multiplexion GmbH), which uses a single nucleotide polymorphism (SNP) typing approach, and was performed as described at www.multiplexion.de. All parental and edited cell lines were regularly tested for *Mycoplasma* contamination using a PCR-based approach and were confirmed to be *Mycoplasma*-free.

Cell culture treatments

To allosterically inhibit mTOR, rapamycin (#S1039, Selleckchem), everolimus (#S1120, Selleckchem) or temsirolimus (# S1044, Selleckchem) were dissolved in DMSO and added directly into full cell culture media at a final concentration of 20 nM unless otherwise indicated in the figure legends. Treatments were performed for the times described in the figure legends. DMSO was used as a negative control for all treatments. Torin1 (#4247, Tocris) was used as an ATP-competitive mTOR inhibitor and added in the culture media at a final concentration of 250 nM for 1 hour.

Amino acid (AA) starvation experiments were performed as described previously (Demetriades *et al*, 2014; Demetriades *et al*, 2016). In brief, custom-made starvation media were formulated

444 according to the Gibco recipe for high-glucose DMEM specifically omitting all AAs. The
445 media were filtered through a 0.22-µm filter device and tested for proper pH and osmolality
446 before use. For the respective AA-replete (+AA) treatment media, commercially available high-
447 glucose DMEM was used (#41965039, Thermo Fisher Scientific). All treatment media were
448 supplemented with 10% dialyzed FBS (dFBS) and 1x Penicillin-Streptomycin (#15140-122,
449 Gibco). For this purpose, FBS was dialyzed against 1x PBS through 3,500 MWCO dialysis
450 tubing. For basal (+AA) conditions, the culture media were replaced with +AA treatment media
451 1 hour before lysis. For amino-acid starvation (–AA), culture media were replaced with
452 starvation media for 1 hour.
453
454 **Antibodies**
455 Antibodies against phospho-p70 S6K (Thr389) (#9205), p70 S6K (#9202 for Fig. 1C,E; #97596
456 for Fig. 1D,F), FLAG (#2368) and mTOR (#2983) were purchased from Cell Signaling
457 Technology. The anti-human tubulin (#T9026) antibody was purchased from Sigma.
458
459 **Plasmid DNA transfections**
460 Plasmid DNA transfections in HEK293FT cells were performed using Effectene transfection
461 reagent (#301425, QIAGEN) according to the manufacturer's instructions.
462
463 **Generation of the gene-edited mTOR^{RR} cell line**
464 The rapamycin-resistant mTOR (mTOR^{RR}) HEK293FT cell line was generated by gene-editing
465 using the pX459-based CRISPR/Cas9 method as described elsewhere (Ran *et al*, 2013). The
466 sgRNA expression vectors were generated by cloning appropriate DNA oligonucleotides
467 (Suppl. Table 8) in the BbsI restriction sites of pX459 (#62988, Addgene). In brief, transfected
468 cells were selected with 3 µg/ml puromycin (#A11138-03, Thermo Fisher Scientific) 48 hours

post-transfection. Single-cell clones were generated by FACS sorting and individual clones were validated by genomic DNA sequencing and functional assays.

Gene expression analysis (RNA-Seq)

To analyze gene expression changes via RNA-seq experiments, total mRNA was isolated using QIAshredder columns (#79656, QIAGEN) and the RNeasy Plus Mini Kit (#74034, QIAGEN) according to the manufacturer's instructions. RNA-seq experiments were performed by the Max Planck Genome Centre (MPGC) Cologne, Germany (https://mpgc.mpipz.mpg.de/home/). RNA quality was assessed with an Agilent Bioanalyzer (Nanochip). Library preparation was done according to NEBNext Ultra™ II Directional RNA Library Prep Kit for Illumina (#E7760L, New England Biolabs) including polyA enrichment and addition the of ERCC RNA spike-ins. Libraries were quality controlled by Agilent TapeStation or LabChip GX or GX Touch (PerkinElmer). Sequencing-by-synthesis was performed on a HiSeq 3000 (Illumina) with single read mode 1 x 150 bp. Data from one representative RNA-seq experiment, out of two independent replicates, are shown in this manuscript. Each experiment was performed from 3 independent biological replicates. The raw data from both RNA-seq experiments are available in the NCBI Sequence Read Archive (see also the Data Availability section).

Cell lysis and immunoblotting

For standard SDS-PAGE and immunoblotting experiments, cells from a well of a 12-well plate were treated as indicated in the figures and lysed in 250 µl of ice-cold Triton lysis buffer (50 mM Tris pH 7.5, 1% Triton X-100, 150 mM NaCl, 50 mM NaF, 2 mM Na-vanadate, 0.011 gr/ml beta-glycerophosphate) supplemented with 1x PhosSTOP phosphatase inhibitors (#4906837001, Roche) and 1x cOmplete protease inhibitors (#11836153001, Roche) for 10 minutes on ice. Samples were clarified by centrifugation (15000 rpm, 10 min, 4 °C) and supernatants were boiled in 1x SDS sample buffer (5x SDS sample buffer: 350 mM Tris-HCl

pH 6.8, 30% glycerol, 600 mM DTT, 12.8% SDS, 0.12% bromophenol blue). Protein samples were subjected to electrophoretic separation on SDS-PAGE and analyzed by standard Western blotting techniques. In brief, proteins were transferred to nitrocellulose membranes (#10600002 or #10600001, Amersham) and stained with 0.2% Ponceau solution (#33427-01, Serva) to confirm equal loading. Membranes were blocked with 5% skim milk powder (#42590, Serva) in PBS-T [1x PBS, 0.1% Tween-20 (#A1389, AppliChem)] for 1 hour at room temperature, washed three times for 10 min with PBS-T and incubated with primary antibodies [1:1000 in PBS-T, 5% bovine serum albumin (BSA; #10735086001, Roche)] rotating overnight at 4 °C. The next day, membranes were washed three times for 10 min with PBS-T and incubated with appropriate HRP-conjugated secondary antibodies (1:10000 in PBS-T, 5% milk) for 1 hour at room temperature. Signals were detected by enhanced chemiluminescence (ECL) using the ECL Western Blotting Substrate (#W1015, Promega) or SuperSignal West Pico PLUS (#34577, Thermo Scientific) and SuperSignal West Femto Substrate (#34095, Thermo Scientific) for weaker signals. Immunoblot images were captured on films (#28906835, GE Healthcare; #4741019289, Fujifilm).

Co-immunoprecipitation (co-IP)

For co-IP experiments, 1.5 x 10^6 cells were transiently transfected with the indicated plasmids and lysed 36 h post-transfection in IP lysis buffer (50 mM Tris pH 7.5, 0.3% CHAPS, 150 mM NaCl, 50 mM NaF, 2 mM Na-vanadate, 0.011 g/ml β-glycerophosphate, 1x PhosSTOP phosphatase inhibitors and 1x cOmplete protease inhibitors). FLAG-tagged proteins were incubated with 30 µl pre-washed anti-FLAG M2 affinity gel (Sigma, #A2220) for 3 h at 4 °C and washed four times with IP wash buffer (50 mM Tris pH 7.5, 0.3% CHAPS, 150 mM NaCl and 50 mM NaF). Samples were then boiled for 6 min in 1x SDS sample buffer and analysed by immunoblotting using appropriate antibodies.

Quantitative whole-cell proteomics

For mass-spectrometry experiments, HEK293FT cells were cultured in 10 cm dishes in 10 ml of complete culture media as described above. Rapamycin (or DMSO as negative control) were added directly in the culture media for 24 or 48 hours. Experiments were performed with 5 independent biological replicates per condition (1x 10 cm dish per replicate). In brief, cells were scraped, collected in 1.5 ml tubes on ice, washed in serum-free media, pelleted by centrifugation (500 x g, 3 min), and cell pellets were snap-frozen in liquid nitrogen and stored at -80 °C.

Sample preparation

For sample preparation for quantitative proteomic analysis, cell pellets were lysed in 6 M guanidinium chloride (GdmCl) supplemented with 2.5 mM TCEP (tris(2-carboxyethyl)phosphine), 10 mM CAA (chloroacetamide) and 100 mM Tris-HCl at room temperature. Samples were boiled at 95 °C for 10 min and sonicated for 30 sec for 10 cycles, with 30 sec breaks on high-performance mode with Bioruptor Plus (#B01020001, Diagenode). Samples were centrifuged at 20000 x g for 20 min at RT, supernatants were diluted 10 times with 20 mM Tris and protein concentration was measured using Nanodrop 2000 (#ND-2000, Thermo Fischer Scientific). Three hundred micrograms of each sample were diluted 10 times with 20 mM Tris and digested with 1.5 µl of Mass Spectrometry Grade Trypsin Gold (#V5280, Promega) at 37 °C overnight. Digestion was stopped by adding 50% FA to the reaction at a final concentration of 1%. Samples were centrifuged at 20000 x g for 10 min at RT and supernatants were collected. C-18-SD StageTips were washed and equilibrated sequentially with 200 µl methanol, 200 µl 40% ACN (acetonitrile) / 0.1% FA (formic acid) and 200 µl 0.1% FA by centrifugation, each step for 1 min at RT. Samples were diluted with 0.1% FA, loaded in StageTips and centrifuged for 1-2 min at RT. StageTips were then washed twice with 200 µl 0.1% FA. Tryptic peptides were eluted from StageTips with 100 µl 40% acetonitrile (ACN) / 0.1% formic acid (FA) by centrifugation (300 x g, 4 min, RT). Eluates were dried in a Speed-

Vac at 45 °C for 40-45 min and resuspended in 20 µl 0.1% FA. Four micrograms of the peptides were dried in a Speed-Vac and stored at -20°C.

TMT10plex labelling

The dried tryptic peptides were reconstituted in 9 µl of 0.1 M TEAB (triethylammonium bicarbonate). Tandem mass tag (TMT10plex; #90110, Thermo Fisher Scientific) labelling was carried out according to the manufacturer's instructions with the following changes: 0.8 mg of TMT10plex reagent was re-suspended with 70 µl anhydrous ACN. Seven microliters of TMT10plex reagent in ACN were added to 9 µl of clean peptide in 0.1 M TEAB. The final ACN concentration was 43.75% and the ratio of peptides to TMT10plex reagent was 1:20. After 60 min incubation, the reaction was quenched with 2 µl 5% hydroxylamine. Labelled peptides were pooled, dried, re-suspended in 200 µl 0.1% FA, split in two equal parts and desalted using home-made STAGE tips (Li *et al*, 2021).

Fractionation of TMT10plex-labeled peptide mixture

One of the two parts was fractionated on a 1 mm x 150 mm ACQUITY column, packed with 130 Å, 1.7 µm C18 particles (#186006935, Waters) using an Ultimate 3000 UHPLC (Thermo Fisher Scientific). Peptides were separated at a flow of 30 µl/min with an 88 min segmented gradient from 1% to 50% buffer B for 85 min and from 50% to 95% buffer B for 3 min; buffer A was 5% ACN, 10 mM ammonium bicarbonate, buffer B was 80% ACN, 10 mM ammonium bicarbonate. Fractions were collected every three minutes, pooled in two passes (fraction 1 + 17, fraction 2 + 18, … , etc.) and dried in a vacuum centrifuge (Eppendorf).

LC-MS/MS analysis

Dried fractions were re-suspended in 0.1% FA, separated on a 50 cm, 75 µm Acclaim PepMap column (#164942, Thermo Fisher Scientific) and analyzed on a Orbitrap Lumos Tribrid mass spectrometer (Thermo Fisher Scientific) equipped with a FAIMS device (Thermo Fisher Scientific). The FAIMS device was operated in two compensation voltages, -50 V and -70 V. Synchronous precursor selection based MS3 was used for the acquisition of the TMT10plex

reporter ion signals. Peptide separations were performed on an EASY-nLC1200 using a 90 min linear gradient from 6% to 31% buffer; buffer A was 0.1% FA, buffer B was 0.1% FA, 80% ACN. The analytical column was operated at 50 °C. Raw files were split based on the FAIMS compensation voltage using FreeStyle (Thermo Fisher Scientific).

Data analysis

Proteomics data was analyzed using MaxQuant, version 1.6.17.0 (Cox & Mann, 2008). The isotope purity correction factors, provided by the manufacturer, were included in the analysis. Differential expression analysis was performed using limma, version 3.34.9 (Ritchie *et al*, 2015) in R, version 3.4.3 (Team, 2017).

Gene Ontology analysis and Data presentation

Gene Ontology (GO) term enrichment analysis was performed using the Database for Annotation, Visualization and Integrated Discovery (DAVID) tool (Huang da *et al*, 2009a, b) of the Flaski toolbox (Iqbal, 2021) (https://flaski.age.mpg.de, developed and provided by the MPI-AGE Bioinformatics core facility). For the RNA-Seq experiments, either all significantly changing genes ($p < 0.05$) or selected genes, whose expression levels changed significantly between rapamycin- and DMSO-treated cells with Log_2-transformed fold change (Log_2FC) values less than -0.75 (downregulated by rapamycin treatment) or higher than +0.8 (upregulated by rapamycin treatment), roughly corresponding to the top and bottom 5% of the dataset, were used for the DAVID GO analysis (for GOTERM_CC_FAT, GOTERM_BP_FAT). The selection criteria for each analysis are described in the respective figure legends.

For the DAVID GO analysis of quantitative proteomics experiments either all significantly changing proteins ($p < 0.05$) or selected proteins whose intensity changes significantly between rapamycin- and DMSO-treated cells with $Log_2FC < -0.55$ and $Log_2FC > +0.4$ (24 h treatments)

598 or $Log_2FC < -0.65$ and $Log_2FC > 0.45$ (48 h treatments) were used (for GOTERM_CC_FAT,
599 GOTERM_BP_FAT). The human proteome was used as reference list for all analyses.
600
601 Cell plots were generated using the DAVID and Cell plot apps in Flaski and include the 15
602 most significant GO terms from each analysis. The full list of genes/proteins that were detected
603 in each experiment (gray dots) was used for generating the Volcano plots. The respective graphs
604 were prepared using the Scatter plot app in Flaski and labelled in Adobe Photoshop (v. 23.4.2).
605 Significantly-changing genes/proteins are represented by blue (downregulated by rapamycin)
606 or red (upregulated by rapamycin) dots. Proteins/genes whose levels change strongly upon
607 rapamycin treatment (based on the selection criteria described above for each experiment) are
608 shown as blue or red dots with black outline.
609
610

Acknowledgements

We thank all members of the Demetriades lab for critical discussions; Sabine Wilhelm for technical support with sample preparation for proteomics; Ilian Athanasov and Xinping Li from the MPI-AGE Proteomics Core Facility for performing the quantitative proteomics experiments described in this study; the Max Planck Genome Centre (MPGC) Cologne (http://mpgc.mpipz.mpg.de/home/) for performing the RNA-seq experiments described in this study; Franziska Metge and Jorge Boucas from the MPI-AGE Bioinformatics Core for initial RNA-Seq analysis; and the MPI-AGE FACS & Imaging Core Facility for support with cell sorting experiments. FA received support by the Cologne Graduate School of Ageing Research (CGA). CD is funded by the European Research Council (ERC) under the European Union's Horizon 2020 research and innovation programme (grant agreement No 757729) and by the Max Planck Society. Illustrations in figures created with BioRender.com.

Author Contributions

Experimental work: FA, NG; data analysis: FA, CD; project design & conceptualization: CD; project supervision: CD; funding acquisition: CD; figure preparation: FA, NG, CD; manuscript draft: FA, CD. All authors approved the final version of the manuscript and agree on the content and conclusions.

Declaration of interests

The authors declare no competing interests.

Data availability

The data that support the findings of this study (uncropped immunoblots) or any additional information required to reanalyze the data reported in this paper are available from the

636 corresponding author upon reasonable request. Other datasets that are produced in this study
637 are available in the following databases:

638 • RNA-Seq data: NCBI Sequence Read Archive (SRA) PRJNA872474
639 (www.ncbi.nlm.nih.gov/sra/PRJNA872474).

640 • Mass spectrometry proteomics: PRIDE (Perez-Riverol *et al*, 2022) PXD038051
641 (www.ebi.ac.uk/pride/archive/projects/PXD038051).

642

643 **Code availability**

644 No code was generated in this study.

645

646 **Additional Information**

647 Supplementary Information (Expanded View Figures 1-4 and Supplementary Tables 1-8) is
648 available for this paper.

649

650 Correspondence and requests for materials should be addressed to Constantinos Demetriades
651 (Demetriades@age.mpg.de).

652

References

(EMA) EMA, 2005. Rapamune: EPAR - Scientific Discussion.

Arriola Apelo SI, Lamming DW (2016) Rapamycin: An InhibiTOR of Aging Emerges From the Soil of Easter Island. *J Gerontol A Biol Sci Med Sci* 71: 841-849

Asrani K, Sood A, Torres A, Georgess D, Phatak P, Kaur H, Dubin A, Talbot CC, Jr., Elhelu L, Ewald AJ *et al* (2017) mTORC1 loss impairs epidermal adhesion via TGF-beta/Rho kinase activation. *J Clin Invest* 127: 4001-4017

Bain J, McLauchlan H, Elliott M, Cohen P (2003) The specificities of protein kinase inhibitors: an update. *Biochem J* 371: 199-204

Bain J, Plater L, Elliott M, Shpiro N, Hastie CJ, McLauchlan H, Klevernic I, Arthur JS, Alessi DR, Cohen P (2007) The selectivity of protein kinase inhibitors: a further update. *Biochem J* 408: 297-315

Bayeva M, Khechaduri A, Puig S, Chang HC, Patial S, Blackshear PJ, Ardehali H (2012) mTOR regulates cellular iron homeostasis through tristetraprolin. *Cell Metab* 16: 645-657

Benjamin D, Colombi M, Moroni C, Hall MN (2011) Rapamycin passes the torch: a new generation of mTOR inhibitors. *Nat Rev Drug Discov* 10: 868-880

Bitto A, Ito TK, Pineda VV, LeTexier NJ, Huang HZ, Sutlief E, Tung H, Vizzini N, Chen B, Smith K *et al* (2016) Transient rapamycin treatment can increase lifespan and healthspan in middle-aged mice. *Elife* 5

Bjedov I, Toivonen JM, Kerr F, Slack C, Jacobson J, Foley A, Partridge L (2010) Mechanisms of life span extension by rapamycin in the fruit fly Drosophila melanogaster. *Cell Metab* 11: 35-46

Bonner JM, Boulianne GL (2017) Diverse structures, functions and uses of FK506 binding proteins. *Cell Signal* 38: 97-105

Brown EJ, Beal PA, Keith CT, Chen J, Shin TB, Schreiber SL (1995) Control of p70 s6 kinase by kinase activity of FRAP in vivo. *Nature* 377: 441-446

Bultynck G, De Smet P, Rossi D, Callewaert G, Missiaen L, Sorrentino V, De Smedt H, Parys JB (2001) Characterization and mapping of the 12 kDa FK506-binding protein (FKBP12)-binding site on different isoforms of the ryanodine receptor and of the inositol 1,4,5-trisphosphate receptor. *Biochem J* 354: 413-422

Castillo-Quan JI, Tain LS, Kinghorn KJ, Li L, Gronke S, Hinze Y, Blackwell TK, Bjedov I, Partridge L (2019) A triple drug combination targeting components of the nutrient-sensing network maximizes longevity. *Proc Natl Acad Sci U S A* 116: 20817-20819

Chen J, Zheng XF, Brown EJ, Schreiber SL (1995) Identification of an 11-kDa FKBP12-rapamycin-binding domain within the 289-kDa FKBP12-rapamycin-associated protein and characterization of a critical serine residue. *Proc Natl Acad Sci U S A* 92: 4947-4951

Chen L, Xu B, Liu L, Liu C, Luo Y, Chen X, Barzegar M, Chung J, Huang S (2015) Both mTORC1 and mTORC2 are involved in the regulation of cell adhesion. *Oncotarget* 6: 7136-7150

Choi J, Chen J, Schreiber SL, Clardy J (1996) Structure of the FKBP12-rapamycin complex interacting with the binding domain of human FRAP. *Science* 273: 239-242

Chung J, Kuo CJ, Crabtree GR, Blenis J (1992) Rapamycin-FKBP specifically blocks growth-dependent activation of and signaling by the 70 kd S6 protein kinases. *Cell* 69: 1227-1236

Cox J, Mann M (2008) MaxQuant enables high peptide identification rates, individualized p.p.b.-range mass accuracies and proteome-wide protein quantification. *Nat Biotechnol* 26: 1367-1372

Creevy KE, Akey JM, Kaeberlein M, Promislow DEL, Dog Aging Project C (2022) An open science study of ageing in companion dogs. *Nature* 602: 51-57

Davies SP, Reddy H, Caivano M, Cohen P (2000) Specificity and mechanism of action of some commonly used protein kinase inhibitors. *Biochem J* 351: 95-105

Davis MI, Hunt JP, Herrgard S, Ciceri P, Wodicka LM, Pallares G, Hocker M, Treiber DK, Zarrinkar PP (2011) Comprehensive analysis of kinase inhibitor selectivity. *Nat Biotechnol* 29: 1046-1051

Demetriades C, Doumpas N, Teleman AA (2014) Regulation of TORC1 in response to amino acid starvation via lysosomal recruitment of TSC2. *Cell* 156: 786-799

Demetriades C, Plescher M, Teleman AA (2016) Lysosomal recruitment of TSC2 is a universal response to cellular stress. *Nat Commun* 7: 10662

Dickinson JM, Fry CS, Drummond MJ, Gundermann DM, Walker DK, Glynn EL, Timmerman KL, Dhanani S, Volpi E, Rasmussen BB (2011) Mammalian target of rapamycin complex 1 activation is required for the stimulation of human skeletal muscle protein synthesis by essential amino acids. *J Nutr* 141: 856-862

Dorrello NV, Peschiaroli A, Guardavaccaro D, Colburn NH, Sherman NE, Pagano M (2006) S6K1- and betaTRCP-mediated degradation of PDCD4 promotes protein translation and cell growth. *Science* 314: 467-471

Dowling RJ, Topisirovic I, Alain T, Bidinosti M, Fonseca BD, Petroulakis E, Wang X, Larsson O, Selvaraj A, Liu Y *et al* (2010) mTORC1-mediated cell proliferation, but not cell growth, controlled by the 4E-BPs. *Science* 328: 1172-1176

Farag SS, Zhang S, Jansak BS, Wang X, Kraut E, Chan K, Dancey JE, Grever MR (2009) Phase II trial of temsirolimus in patients with relapsed or refractory multiple myeloma. *Leuk Res* 33: 1475-1480

717 Fedorov O, Marsden B, Pogacic V, Rellos P, Muller S, Bullock AN, Schwaller J, Sundstrom M, Knapp
718 S (2007) A systematic interaction map of validated kinase inhibitors with Ser/Thr kinases. *Proc Natl*
719 *Acad Sci U S A* 104: 20523-20528

720 Fernandes SA, Demetriades C (2021) The Multifaceted Role of Nutrient Sensing and mTORC1
721 Signaling in Physiology and Aging. *Front Aging* 2: 707372

722 Fok WC, Chen Y, Bokov A, Zhang Y, Salmon AB, Diaz V, Javors M, Wood WH, 3rd, Zhang Y, Becker
723 KG *et al* (2014) Mice fed rapamycin have an increase in lifespan associated with major changes in the
724 liver transcriptome. *PLoS One* 9: e83988

725 Fonseca BD, Smith EM, Yelle N, Alain T, Bushell M, Pause A (2014) The ever-evolving role of mTOR
726 in translation. *Semin Cell Dev Biol* 36: 102-112

727 Fries GR, Gassen NC, Rein T (2017) The FKBP51 Glucocorticoid Receptor Co-Chaperone: Regulation,
728 Function, and Implications in Health and Disease. *Int J Mol Sci* 18

729 Galfre E, Pitt SJ, Venturi E, Sitsapesan M, Zaccai NR, Tsaneva-Atanasova K, O'Neill S, Sitsapesan R
730 (2012) FKBP12 activates the cardiac ryanodine receptor Ca2+-release channel and is antagonised by
731 FKBP12.6. *PLoS One* 7: e31956

732 Ge Y, Wu AL, Warnes C, Liu J, Zhang C, Kawasome H, Terada N, Boppart MD, Schoenherr CJ, Chen
733 J (2009) mTOR regulates skeletal muscle regeneration in vivo through kinase-dependent and kinase-
734 independent mechanisms. *Am J Physiol Cell Physiol* 297: C1434-1444

735 Goodman CA, Frey JW, Mabrey DM, Jacobs BL, Lincoln HC, You JS, Hornberger TA (2011) The role
736 of skeletal muscle mTOR in the regulation of mechanical load-induced growth. *J Physiol* 589: 5485-
737 5501

738 Gordon EB, Hart GT, Tran TM, Waisberg M, Akkaya M, Skinner J, Zinocker S, Pena M, Yazew T, Qi
739 CF *et al* (2015) Inhibiting the Mammalian target of rapamycin blocks the development of experimental
740 cerebral malaria. *mBio* 6: e00725

741 Graber TG, Borack MS, Reidy PT, Volpi E, Rasmussen BB (2017) Essential amino acid ingestion alters
742 expression of genes associated with amino acid sensing, transport, and mTORC1 regulation in human
743 skeletal muscle. *Nutr Metab (Lond)* 14: 35

744 Hantschel O (2015) Unexpected off-targets and paradoxical pathway activation by kinase inhibitors.
745 *ACS Chem Biol* 10: 234-245

746 Hantschel O, Grebien F, Superti-Furga G (2012) The growing arsenal of ATP-competitive and allosteric
747 inhibitors of BCR-ABL. *Cancer Res* 72: 4890-4895

748 Hara K, Yonezawa K, Kozlowski MT, Sugimoto T, Andrabi K, Weng QP, Kasuga M, Nishimoto I,
749 Avruch J (1997) Regulation of eIF-4E BP1 phosphorylation by mTOR. *J Biol Chem* 272: 26457-26463

Hardwick JS, Kuruvilla FG, Tong JK, Shamji AF, Schreiber SL (1999) Rapamycin-modulated transcription defines the subset of nutrient-sensitive signaling pathways directly controlled by the Tor proteins. *Proc Natl Acad Sci U S A* 96: 14866-14870

Harrar Y, Bellini C, Faure JD (2001) FKBPs: at the crossroads of folding and transduction. *Trends Plant Sci* 6: 426-431

Harrison DE, Strong R, Sharp ZD, Nelson JF, Astle CM, Flurkey K, Nadon NL, Wilkinson JE, Frenkel K, Carter CS *et al* (2009) Rapamycin fed late in life extends lifespan in genetically heterogeneous mice. *Nature* 460: 392-395

Holz MK, Ballif BA, Gygi SP, Blenis J (2005) mTOR and S6K1 mediate assembly of the translation preinitiation complex through dynamic protein interchange and ordered phosphorylation events. *Cell* 123: 569-580

Hosoi H, Dilling MB, Shikata T, Liu LN, Shu L, Ashmun RA, Germain GS, Abraham RT, Houghton PJ (1999) Rapamycin causes poorly reversible inhibition of mTOR and induces p53-independent apoptosis in human rhabdomyosarcoma cells. *Cancer Res* 59: 886-894

Huang da W, Sherman BT, Lempicki RA (2009a) Bioinformatics enrichment tools: paths toward the comprehensive functional analysis of large gene lists. *Nucleic Acids Res* 37: 1-13

Huang da W, Sherman BT, Lempicki RA (2009b) Systematic and integrative analysis of large gene lists using DAVID bioinformatics resources. *Nat Protoc* 4: 44-57

Hudes G, Carducci M, Tomczak P, Dutcher J, Figlin R, Kapoor A, Staroslawska E, Sosman J, McDermott D, Bodrogi I *et al* (2007) Temsirolimus, interferon alfa, or both for advanced renal-cell carcinoma. *N Engl J Med* 356: 2271-2281

Huo Y, Iadevaia V, Proud CG (2011) Differing effects of rapamycin and mTOR kinase inhibitors on protein synthesis. *Biochem Soc Trans* 39: 446-450

Iqbal A, Duitama, Camila, Metge, Franziska, Rosskopp, Daniel, & Boucas, Jorge. (2021) Flaski (2.0.0). *Zenodo*

Jin C, Zhao Y, Yu L, Xu S, Fu G (2013) MicroRNA-21 mediates the rapamycin-induced suppression of endothelial proliferation and migration. *FEBS Lett* 587: 378-385

Karaman MW, Herrgard S, Treiber DK, Gallant P, Atteridge CE, Campbell BT, Chan KW, Ciceri P, Davis MI, Edeen PT *et al* (2008) A quantitative analysis of kinase inhibitor selectivity. *Nat Biotechnol* 26: 127-132

Kim JH, Lee C, Lee M, Wang H, Kim K, Park SJ, Yoon I, Jang J, Zhao H, Kim HK *et al* (2017) Control of leucine-dependent mTORC1 pathway through chemical intervention of leucyl-tRNA synthetase and RagD interaction. *Nat Commun* 8: 732

783 Ko JH, Yoon SO, Lee HJ, Oh JY (2017) Rapamycin regulates macrophage activation by inhibiting
784 NLRP3 inflammasome-p38 MAPK-NFkappaB pathways in autophagy- and p62-dependent manners.
785 *Oncotarget* 8: 40817-40831

786 Kolos JM, Voll AM, Bauder M, Hausch F (2018) FKBP Ligands-Where We Are and Where to Go?
787 *Front Pharmacol* 9: 1425

788 Laplante M, Sabatini DM (2013) Regulation of mTORC1 and its impact on gene expression at a glance.
789 *J Cell Sci* 126: 1713-1719

790 Lee J, Moir RD, McIntosh KB, Willis IM (2012) TOR signaling regulates ribosome and tRNA synthesis
791 via LAMMER/Clk and GSK-3 family kinases. *Mol Cell* 45: 836-843

792 Lelegren M, Liu Y, Ross C, Tardif S, Salmon AB (2016) Pharmaceutical inhibition of mTOR in the
793 common marmoset: effect of rapamycin on regulators of proteostasis in a non-human primate. *Pathobiol*
794 *Aging Age Relat Dis* 6: 31793

795 Li J, Kim SG, Blenis J (2014) Rapamycin: one drug, many effects. *Cell Metab* 19: 373-379

796 Li X, Franz T, Atanassov I, Colby T (2021) Step-by-Step Sample Preparation of Proteins for Mass
797 Spectrometric Analysis. *Methods Mol Biol* 2261: 13-23

798 Liu GY, Sabatini DM (2020) mTOR at the nexus of nutrition, growth, ageing and disease. *Nat Rev Mol*
799 *Cell Biol* 21: 183-203

800 Lorenz MC, Heitman J (1995) TOR mutations confer rapamycin resistance by preventing interaction
801 with FKBP12-rapamycin. *J Biol Chem* 270: 27531-27537

802 Luo Y, Liu L, Wu Y, Singh K, Su B, Zhang N, Liu X, Shen Y, Huang S (2015) Rapamycin inhibits
803 mSin1 phosphorylation independently of mTORC1 and mTORC2. *Oncotarget* 6: 4286-4298

804 Ma XM, Blenis J (2009) Molecular mechanisms of mTOR-mediated translational control. *Nat Rev Mol*
805 *Cell Biol* 10: 307-318

806 Martinez NJ, Chang HM, Borrajo Jde R, Gregory RI (2013) The co-chaperones Fkbp4/5 control
807 Argonaute2 expression and facilitate RISC assembly. *RNA* 19: 1583-1593

808 Marz AM, Fabian AK, Kozany C, Bracher A, Hausch F (2013) Large FK506-binding proteins shape
809 the pharmacology of rapamycin. *Mol Cell Biol* 33: 1357-1367

810 Mauvoisin D, Rocque G, Arfa O, Radenne A, Boissier P, Mounier C (2007) Role of the PI3-kinase/mTor
811 pathway in the regulation of the stearoyl CoA desaturase (SCD1) gene expression by insulin in liver. *J*
812 *Cell Commun Signal* 1: 113-125

813 Mayer C, Grummt I (2006) Ribosome biogenesis and cell growth: mTOR coordinates transcription by
814 all three classes of nuclear RNA polymerases. *Oncogene* 25: 6384-6391

Meier-Kriesche HU, Kaplan B (2000) Toxicity and efficacy of sirolimus: relationship to whole-blood concentrations. *Clin Ther* 22 Suppl B: B93-100

Morita M, Prudent J, Basu K, Goyon V, Katsumura S, Hulea L, Pearl D, Siddiqui N, Strack S, McGuirk S *et al* (2017) mTOR Controls Mitochondrial Dynamics and Cell Survival via MTFP1. *Mol Cell* 67: 922-935 e925

Nachef M, Ali AK, Almutairi SM, Lee SH (2021) Targeting SLC1A5 and SLC3A2/SLC7A5 as a Potential Strategy to Strengthen Anti-Tumor Immunity in the Tumor Microenvironment. *Front Immunol* 12: 624324

Nandagopal N, Roux PP (2015) Regulation of global and specific mRNA translation by the mTOR signaling pathway. *Translation (Austin)* 3: e983402

Partridge L, Fuentealba M, Kennedy BK (2020) The quest to slow ageing through drug discovery. *Nat Rev Drug Discov* 19: 513-532

Perez-Riverol Y, Bai J, Bandla C, Garcia-Seisdedos D, Hewapathirana S, Kamatchinathan S, Kundu DJ, Prakash A, Frericks-Zipper A, Eisenacher M *et al* (2022) The PRIDE database resources in 2022: a hub for mass spectrometry-based proteomics evidences. *Nucleic Acids Res* 50: D543-D552

Powers RW, 3rd, Kaeberlein M, Caldwell SD, Kennedy BK, Fields S (2006) Extension of chronological life span in yeast by decreased TOR pathway signaling. *Genes Dev* 20: 174-184

Powers T, Walter P (1999) Regulation of ribosome biogenesis by the rapamycin-sensitive TOR-signaling pathway in Saccharomyces cerevisiae. *Mol Biol Cell* 10: 987-1000

Ramanathan A, Schreiber SL (2009) Direct control of mitochondrial function by mTOR. *Proc Natl Acad Sci U S A* 106: 22229-22232

Ran FA, Hsu PD, Wright J, Agarwala V, Scott DA, Zhang F (2013) Genome engineering using the CRISPR-Cas9 system. *Nat Protoc* 8: 2281-2308

Ritchie ME, Phipson B, Wu D, Hu Y, Law CW, Shi W, Smyth GK (2015) limma powers differential expression analyses for RNA-sequencing and microarray studies. *Nucleic Acids Res* 43: e47

Robida-Stubbs S, Glover-Cutter K, Lamming DW, Mizunuma M, Narasimhan SD, Neumann-Haefelin E, Sabatini DM, Blackwell TK (2012) TOR signaling and rapamycin influence longevity by regulating SKN-1/Nrf and DAF-16/FoxO. *Cell Metab* 15: 713-724

Rosario FJ, Gupta MB, Myatt L, Powell TL, Glenn JP, Cox L, Jansson T (2019) Mechanistic Target of Rapamycin Complex 1 Promotes the Expression of Genes Encoding Electron Transport Chain Proteins and Stimulates Oxidative Phosphorylation in Primary Human Trophoblast Cells by Regulating Mitochondrial Biogenesis. *Sci Rep* 9: 246

847 Schieke SM, Phillips D, McCoy JP, Jr., Aponte AM, Shen RF, Balaban RS, Finkel T (2006) The
848 mammalian target of rapamycin (mTOR) pathway regulates mitochondrial oxygen consumption and
849 oxidative capacity. *J Biol Chem* 281: 27643-27652

850 Schinaman JM, Rana A, Ja WW, Clark RI, Walker DW (2019) Rapamycin modulates tissue aging and
851 lifespan independently of the gut microbiota in Drosophila. *Sci Rep* 9: 7824

852 Sun L, Yan Y, Lv H, Li J, Wang Z, Wang K, Wang L, Li Y, Jiang H, Zhang Y (2022) Rapamycin targets
853 STAT3 and impacts c-Myc to suppress tumor growth. *Cell Chem Biol* 29: 373-385 e376

854 Takasaki S, Yamaguchi H, Kawasaki Y, Kikuchi M, Tanaka M, Ito A, Mano N (2019) Long-term
855 relationship between everolimus blood concentration and clinical outcomes in Japanese patients with
856 metastatic renal cell carcinoma: a prospective study. *J Pharm Health Care Sci* 5: 6

857 Tardif S, Ross C, Bergman P, Fernandez E, Javors M, Salmon A, Spross J, Strong R, Richardson A
858 (2015) Testing efficacy of administration of the antiaging drug rapamycin in a nonhuman primate, the
859 common marmoset. *J Gerontol A Biol Sci Med Sci* 70: 577-587

860 Team RC (2017) R Core Team (2017) R: A Language and Environment for Statistical Computing.

861 Thoreen CC, Chantranupong L, Keys HR, Wang T, Gray NS, Sabatini DM (2012) A unifying model
862 for mTORC1-mediated regulation of mRNA translation. *Nature* 485: 109-113

863 Thoreen CC, Kang SA, Chang JW, Liu Q, Zhang J, Gao Y, Reichling LJ, Sim T, Sabatini DM, Gray
864 NS (2009) An ATP-competitive mammalian target of rapamycin inhibitor reveals rapamycin-resistant
865 functions of mTORC1. *J Biol Chem* 284: 8023-8032

866 Torrence ME, MacArthur MR, Hosios AM, Valvezan AJ, Asara JM, Mitchell JR, Manning BD (2021)
867 The mTORC1-mediated activation of ATF4 promotes protein and glutathione synthesis downstream of
868 growth signals. *Elife* 10

869 Tsukumo Y, Alain T, Fonseca BD, Nadon R, Sonenberg N (2016) Translation control during prolonged
870 mTORC1 inhibition mediated by 4E-BP3. *Nat Commun* 7: 11776

871 Urfer SR, Kaeberlein TL, Mailheau S, Bergman PJ, Creevy KE, Promislow DEL, Kaeberlein M (2017)
872 A randomized controlled trial to establish effects of short-term rapamycin treatment in 24 middle-aged
873 companion dogs. *Geroscience* 39: 117-127

874 Vervliet T, Parys JB, Bultynck G (2015) Bcl-2 and FKBP12 bind to IP3 and ryanodine receptors at
875 overlapping sites: the complexity of protein-protein interactions for channel regulation. *Biochem Soc*
876 *Trans* 43: 396-404

877 Villa-Cuesta E, Holmbeck MA, Rand DM (2014) Rapamycin increases mitochondrial efficiency by
878 mtDNA-dependent reprogramming of mitochondrial metabolism in Drosophila. *J Cell Sci* 127: 2282-
879 2290

Visner GA, Lu F, Zhou H, Liu J, Kazemfar K, Agarwal A (2003) Rapamycin induces heme oxygenase-1 in human pulmonary vascular cells: implications in the antiproliferative response to rapamycin. *Circulation* 107: 911-916

Wall M, Poortinga G, Hannan KM, Pearson RB, Hannan RD, McArthur GA (2008) Translational control of c-MYC by rapamycin promotes terminal myeloid differentiation. *Blood* 112: 2305-2317

Wang R, Yu Z, Sunchu B, Shoaf J, Dang I, Zhao S, Caples K, Bradley L, Beaver LM, Ho E *et al* (2017) Rapamycin inhibits the secretory phenotype of senescent cells by a Nrf2-independent mechanism. *Aging Cell* 16: 564-574

Wang T, Li BY, Danielson PD, Shah PC, Rockwell S, Lechleider RJ, Martin J, Manganaro T, Donahoe PK (1996) The immunophilin FKBP12 functions as a common inhibitor of the TGF beta family type I receptors. *Cell* 86: 435-444

Wang X, Yue P, Chan CB, Ye K, Ueda T, Watanabe-Fukunaga R, Fukunaga R, Fu H, Khuri FR, Sun SY (2007) Inhibition of mammalian target of rapamycin induces phosphatidylinositol 3-kinase-dependent and Mnk-mediated eukaryotic translation initiation factor 4E phosphorylation. *Mol Cell Biol* 27: 7405-7413

Zaragoza D, Ghavidel A, Heitman J, Schultz MC (1998) Rapamycin induces the G0 program of transcriptional repression in yeast by interfering with the TOR signaling pathway. *Mol Cell Biol* 18: 4463-4470

Zhang H, Stallock JP, Ng JC, Reinhard C, Neufeld TP (2000) Regulation of cellular growth by the Drosophila target of rapamycin dTOR. *Genes Dev* 14: 2712-2724

Zhang X, Chen W, Gao Q, Yang J, Yan X, Zhao H, Su L, Yang M, Gao C, Yao Y *et al* (2019) Rapamycin directly activates lysosomal mucolipin TRP channels independent of mTOR. *PLoS Biol* 17: e3000252

Zhang Y, Swanda RV, Nie L, Liu X, Wang C, Lee H, Lei G, Mao C, Koppula P, Cheng W *et al* (2021) mTORC1 couples cyst(e)ine availability with GPX4 protein synthesis and ferroptosis regulation. *Nat Commun* 12: 1589

Zhu Y, Zou R, Sha H, Lu Y, Zhang Y, Wu J, Feng J, Wang D (2020) Lipid metabolism-related proteins of relevant evolutionary and lymphoid interest (PRELI) domain containing family proteins in cancer. *Am J Transl Res* 12: 6015-6026